

Carrier Phase Delay Altimetry from Low Elevation GPSR Measurements

Estel Cardellach^{*2}, Robert Treuhaff¹, Garth Franklin¹, Jacob Gorelik¹, Stephen T. Lowe¹ and Lawrence E. Young¹

¹NASA/JPL Jet Propulsion Laboratory, California Institute of Technology, Pasadena, USA, <http://www.jpl.nasa.gov>

²NRC associate at NASA/JPL

Abstract

GPS-Reflections (GPSR) observations at very low elevation angles take advantage of the apparent smoothness of the surface to enable phase-delay altimetry, of centimetric nominal precision, higher than the GPSR code-delay estimates. The potential applications of this grazing technique include coastal monitoring from the ground, as well as aircraft and spaceborne bistatic altimetric measurements over the ocean. Low-elevation coastal measurements potentially enable nearly continuous monitoring of eddies within 20 km of the coast, using receivers on mountains or towers. Spaceborne measurements at low-elevation, coherent signals might reduce or obviate the need for high-gain receiving antennas. The limitations of this technique, however, have never been assessed. This presentation tackles the surface roughness effects as well as the delay and bending impact of the troposphere. Coastal experimental data together with sea surface, atmospheric ray tracing and electromagnetic models and simulations have been used to quantify dominant elements of the error budget of the phase-delay GPSR altimetric products at low elevation.

Keywords: GNSS-R, Altimetry, Remote Sensing, GPS, Galileo

1. Introduction

The Global Positioning System (GPS) provides free, global and permanent coverage of L band double frequency coded signals. The signals' characteristics together with the current inexpensiveness of the receiver technology, makes the GPS signal a good candidate to source of opportunity for passive remote-sensing of the Earth. Actually, areas such as tectonic, ionospheric and tropospheric monitoring are already taking advantage of this source. The possibility of using the bistatic reflections of the GPS signal onto the oceans' surface (GPSR) was described in (Martín-Neira, M., 1993), and for the last decade, several experimental results have been published, reporting scatterometric and altimetric capabilities of the GPSR technique. The retrieval of wind and roughness properties of the sea surface from aircraft and high altitude balloons have

* Corresponding author, email: Estel.Cardellach@jpl.nasa.gov

been displayed (Zavorotny and Voronovich, 2000), (Garrison et al., 2002), or (Cardellach et al., 2003). GPSR have also been obtained from space-based receivers (Lowe et al., 2002), (Beyerle et al., 2002). On the other hand, the altimetric performance from air-borne receivers has been proved to be of 5-cm precision, (Lowe et al., 2002b), using the group delay observables derived from the encrypted P(Y) code of the GPS signal from 2 satellites and 7-km resolution. In order to achieve few centimeters precision in a single transmitter-receiver link, and thus make the most of the coverage capabilities of the system, it is required to use the carrier phase measurements. This transition, from group delay to carrier phase delay for obtaining better precision was also done in other technologies such as VLBI or direct positioning with GPS.

(Treuhaft et al., 2001) and (Martín-Neira et al., 2001) reported GPSR carrier-phase measurements with centimetric precision. In both cases the reflecting water surface was not the open sea, but smoother surfaces with undulations below the GPS wavelength. The roughness of the open sea surface, however, is much greater than the carrier wavelengths, making the reflection an essentially diffuse process, with very low coherence at most elevations. A possible way to achieve higher coherence is to descend to grazing angles of observation, from which the surface appears smoother. Nevertheless, the same procedure that provides smoother surface also induces a large error in the vertical, altimetric, component when the slant delay has a small uncertainty. Is it worth to descend to grazing angles? If we can track the interferometric carrier phase with 5 degrees uncertainty, the vertical error of a single 0.02 seconds observation at 1° elevation would result 15 cm, higher precision than a single code observation at nadir (of the order of the meter).

If the technique could be applied on the open sea, it would be indeed possible to imagine a cheap technology for monitoring the mesoscale coastal dynamic structures from cliffs, towers or buildings close to the sea, where the current observation system have important gaps in the coverage of the such coastal areas (instruments' footprint polluted by the mainland), as well as in the revisiting time. The coastal GPSR measurements would fill both time and space gaps, providing continuous surveys at any desired location. Besides, the technique could be also useful from air-borne and space-borne platforms, although the results presented in this paper have been computed from data and simulations at lower altitudes.

The main purpose of this paper is to report the existence of carrier coherence and the possibility of interferometric phase GPSR techniques on the open sea, even with surface waves much larger than the electro-magnetic carrier wavelengths. We also aim to identify some major effects on the signal that could introduce noise and errors, to begin to construct the error budget for the GPSR low elevation altimetric measurements.

2. Data set and pre-processing

We present results from a GPSR data set recorded in September 2002 in Palos Verdes, California, USA. A 30° beam antenna was located on top of a ~ 85 m high bluff,

pointing to the horizon above the ocean (Figure 1). The output of the antenna front end was down converted and recorded at 20.4 Mbps during occultations of GPS satellites.



Figure 1: Picture of the antennas used in Palos Verdes, September 2002. The GPSR antenna for low elevation measurements is the square patch facing the ocean. An omnidirectional, zenith-looking choke-ring antenna was also located on the site to collect geodetic/tropospheric data. The site was at ~85 m above the sea level.

The raw data stream is then cross-correlated with a model of the signal (known Pseudo Random Noise--PRN--code of the corresponding satellite modulating a carrier field with estimable Doppler frequency), to produce and store the correlation function for ~60 lags (called waveform or delay-waveform hereafter). Both direct and reflected branches of the signal are present in the data stream, delayed by the difference between the reflected and the direct travel time as $(r_r - r_d)/c$ (r_r and r_d read as the specular-reflected and direct trajectory length respectively). If the reflecting surface was smooth to produce specular reflection, those two delayed rays would be the only components of the signal modulated by a given PRN. Otherwise, when the vertical scales of the roughness are greater than the GPS L1 wavelength λ , we expect to find other further delayed contributions from multipath of the signal onto the rough features of the surface. The complex waveform for a given delay-lag τ_i with respect to the direct arrival time τ_0 should follow the shape:

$$A(\tau_i) = e^{i\phi_0} [A_d \Delta(\tau_i - \tau_0) + A_r e^{ik_0(r_r - r_d)} \Delta(\tau_i - \tau_0 - (r_r - r_d)/c) + \sum_{secondary\ refl-r_j} A_{r_j} e^{ik_0(r_j - r_d)} \Delta(\tau_i - \tau_0 - (r_j - r_d)/c)] + noise \quad [1]$$

Being A_d and A_r the amplitude of correlation due to the direct and reflected components of the signal; k_0 the GPS L1 wavenumber; $\Delta(\tau)$ the triangle function GPS autocorrelation function at delay τ ; ϕ_0 an initial phase; c the speed of the light; and $\sum_{secondary\ refl-r_j}$ are the bunch of contributions from secondary reflection processes with a ray trajectory length $r_{r_j} > r_r$, and potentially $r_{r_j} - r_r > \lambda$. Therefore, assuming specular reflection, the function reduces to (Treuhaft et al., 2001):

$$A(\tau_i) = e^{i\phi_0} [A_d \Delta(\tau_i - \tau_0) + A_r e^{ik_0(r_r - r_d)} \Delta(\tau_i - \tau_0 - (r_r - r_d)/c)] + noise \quad [2]$$

3. Coherence of the signal

The assumption of the paper is that the surface appears smooth enough to behave as a specular reflector at low elevation angles of observation. If so, Equation 2 should apply, yielding an interferometric fringe. Note that if secondary reflection effects are important, random-phase contributions ($ko(rr-rd)-ko(rrj-rd) > 2\pi$) are being added to the total field $A(\tau_j)$, destroying the interferometric pattern. Therefore, the existence of an interferometric fringe may be used to check the coherence of the reflection. As displayed in Figure 2, the amplitude of the signals collected by the horizon-looking antenna oscillate with a period of several seconds, and this fringe is gradually destroyed for rising angles of observation.

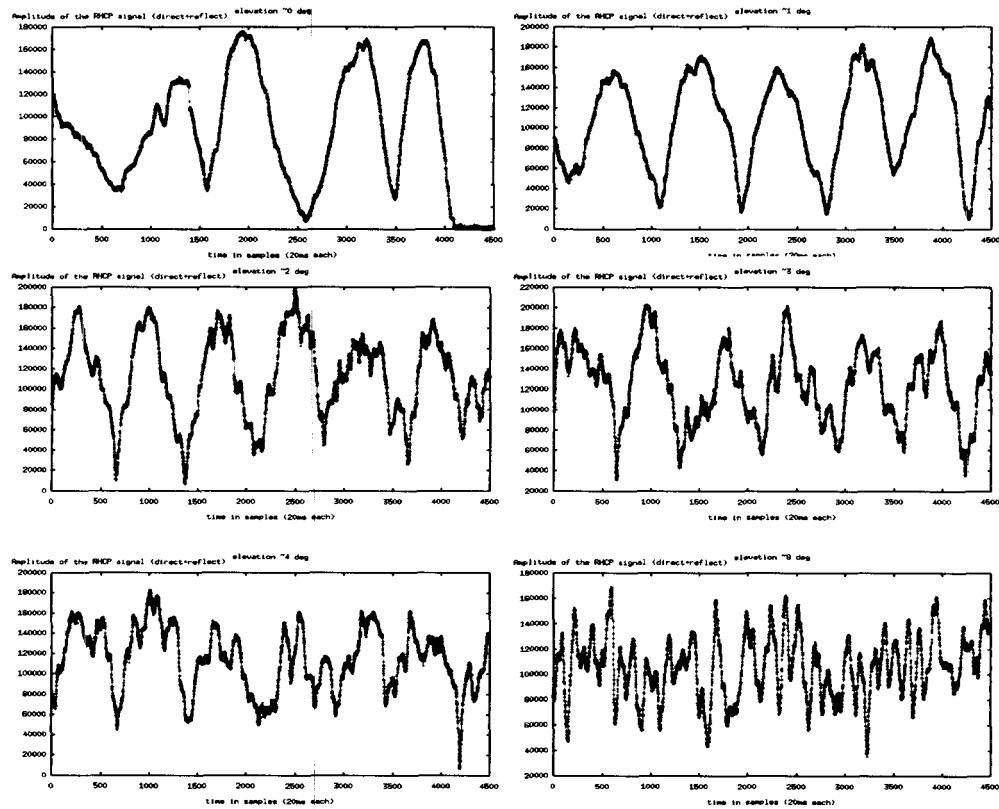


Figure 2: Amplitude of the total field reaching the antenna, PRN13 and six angles of observation (from top to bottom and left to right: ~0,~1,~2,~3,~4 and ~8 degrees elevation). The time-axis corresponds to 90 seconds (20 ms/observation). The interference between the direct and the reflected signal produces a neat fringe at very low elevation, whereas random components destroy it gradually as the observation angle rises.

The frequency of the amplitude's beats should be the time variation of the interferometric phase ($k_0(rr-rd)$ in Equation 2). Assuming the reflected-to-direct delay ($rr-rd$) expressed in units of carrier cycles as

$$(rr-rd) = 2 H \sin(el) / \lambda + D_{trop} + D_{rough} + D_{others} \quad [3]$$

(H for altitude of the receiver with respect to the reflecting surface; D_{trop} , D_{rough} and D_{others} for excess of delay in the reflected signal introduced by the troposphere, roughness and other sources respectively, in units of cycles). The frequency becomes

$$f = 2 H \cos(el) / \lambda \, del/dt + 2 \sin(el) / \lambda \, dH/dt + dD_{trop}/dt + dD_{rough}/dt + dD_{others}/dt \quad [4]$$

For periods of time of the order of few minutes, the mean altitude of the static receiver may be considered as a constant value, if the surface is assumed effectively smooth. The frequency of the amplitude oscillations, when neglecting the corrective terms, then reads

$$f = 2 H \cos(el) / \lambda \, del/dt \quad [5]$$

Since the rate of change of the elevation is almost constant in the range of angles of observation of the current experiment, the frequency is expected to drop as $\cos(el)$. The analysis of the frequency components in the amplitude time series, however, shows a clear acceleration of the interferometric fringe as the elevation rises (Figure 4, red marks). In order to conclude about the nature of the oscillations of the amplitude, and so about the coherent scattering process at low elevation, we need to find out about this unexpected frequency pattern. The effect of the corrective terms have been investigated. In particular, the possible acceleration due to the troposphere and the role of the roughness of the sea surface.

4. Effect of the troposphere

A forward ray tracing model has been implemented to check the effect of the propagation through the low atmosphere, because tropospheric mapping functions in the open literature may not work appropriately at grazing angles, where the gradients of refractivity may bend the ray trajectory with substantial differences in the total delay experience by the signal or location of the specular point. We used an exponential model for the refractivity, with 10 km of vertical scale onto a 2-dimensional round Earth surrounded by a set of 2000 concentric round layers of 20 km total thickness. The error in the reflected-to-direct relative delay with respect to the simple geometric model (first term in Equation 3) has been computed as a function of the elevation. The effect of variations of 20% in the refractivity have been also assessed, in addition to variations in the altitude of the receiver. Figure 3 contains the simulated tropospheric error, understanding "tropospheric error" as the correction to be added in Equation 3, in dimension of length, cycle units:

$$D_{trop} = (rr-rd)_{\{through\ tropo\}} - 2 H \sin(el) / \lambda \quad [7]$$

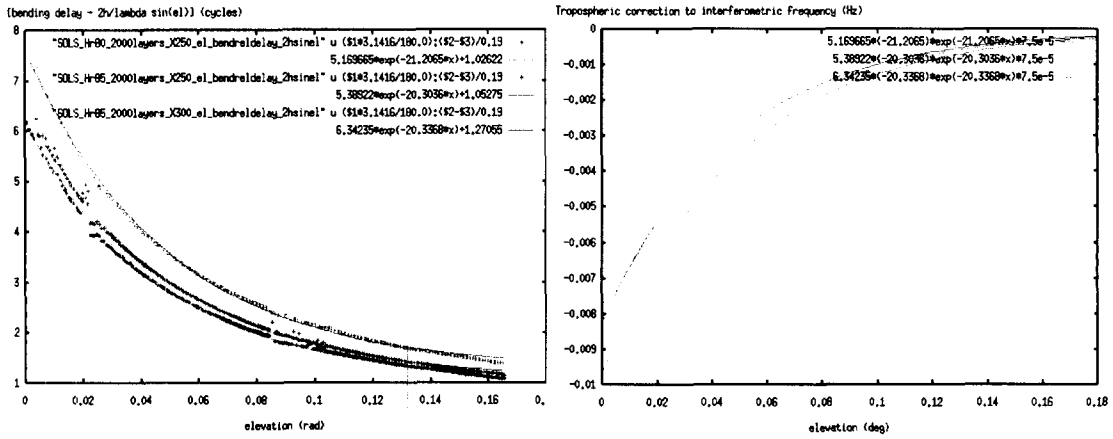


Figure 3: (left) Tropospheric correction, D_{trop} , to be added in Equation 3, as given by ray tracing simulations. 0-level refractivity of 250E-6 and 300E-6 have been used, while the altitude of the receiver has been changed from 85 to 80 meters above the sea surface. An exponential fit to the data has been applied to facilitate the time derivation. (right) Time derivative of the tropospheric error from the exponential fits on the left-plot and a standard value for the elevation rate ($7.5E-5$ rad/sec). Therefore, the plot on the left is the correction that should be added to the interferometric frequency, dD_{trop}/dt in Equation 4 [errata: X-axis is in radians, not degrees].

The simulations indicate that the troposphere slows down the interferometric phase, but with positive slope, speeding it up as elevation rises. This pattern matches the behaviour of the data set, as displayed in Figure 4, supporting the conclusion that the oscillations in the amplitude of the total field are due to the interferometric process between the direct and the reflected signal (coherent scattering), but modulated by the troposphere. The simulations show that an error of 1 m in the a-priori altitude of the receiver would give an error of the order of 1 cm in the tropospheric correction (at 0 degree elevation), whereas an error of 20% in the refractivity introduce 15% error in the correction. These numbers correspond to a static receiver at ~85 m altitude, no other altitudes have been investigated. The interferometric frequency, however, is essentially biased by small variations in the altitude of the receiver (Figure 3b is the frequency correction, to be added to Equation 5, proportional to H), but it preserves the frequency rate of change, while a variation on the refractivity will translate to a different frequency-elevation pattern. Moreover, the frequency features may be used to obtain a coarse estimate of the altimetric range, even with poor knowledge of the atmospheric refractivity. We have corrected the frequency profile and inverted it to obtain H by means of each of the three simulated tropospheric corrections. The results of such coarse inversion are summarized in Table 1, they provide an accuracy of ~1.5m. This accuracy is enough to be used, later, as an a-priori to solve for the cycle ambiguity in the precise inversion of the carrier-phase, since at grazing observations the addition of a cycle results in a variation of the altimetric range bigger than this accuracy level.

| F_trop correction | H estimate [m] |
|-------------------|----------------|
| Hr=80m, Xo=250e-6 | 86.17 +- 1.37 |
| Hr=85m, Xo=250e-6 | 86.11 +- 1.38 |
| Hr=85m, Xo=300e-6 | 87.70 +- 1.34 |

Table 1: Coarse estimation of the altimetric range, H , from the elevation dependency of the interferometric frequency. The accuracy is better than 2 meters, enough to solve the cycle ambiguity in the later inversion of the carrier-phase.

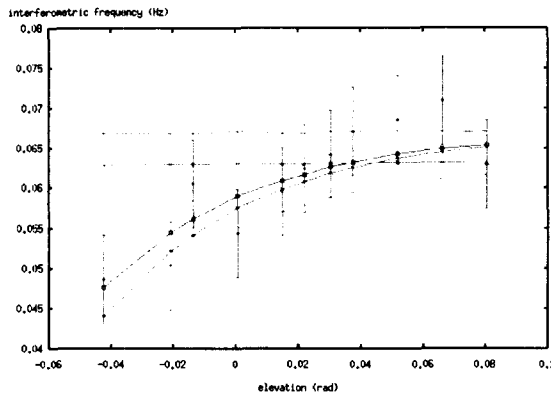


Figure 4: Frequency analysis of the amplitude of the total field (red diamonds). Expected pattern according to Equation 5 (green for 85 m receiver altitude, pink for 80 m height). The interferometric frequency corrected by the tropospheric effect is plot in dark blue (85m, 250E-6 refractivity), brown (85m, 300E-6) and cyan (80m, 250E-6). An exponential fit to the data is plotted in orange.

4. Effect of the roughness

As discussed in (Beckmann and Spizzichino, 1963), the reflection occurs on a zone over the surface usually called glistening zone: the area where the probability of forwarding the signal toward the receiver's direction is significant. The signals rebounded in those other locations, distant to the specular point, have a positive delay with respect to the specular ray path. It may be seen as multipath from other facets of the reflecting surface. (Elfouhaily et al., 2002) give an analytical expression for the additional delay introduced by this effect, dependent on the geometrical delay itself, the elevation of observation and the roughness. This effect has been reported from experimental data in (Rius et al, 2002). For isotropic surface with waves' slope covariance κ , the delay introduced by the roughness becomes (Elfouhaily et al., 2002, Equation 35a)

$$D_{roughness} = 2 H \sin(el) \kappa (1 + 1 / \sin(el)^2) \quad [8]$$

According to this formula, for a given receiver altitude and sea state, the roughness correction would increase as elevation sets. This feature is opposite to the main hypothesis of the paper, for which low elevation provides coherent scattering (sole specular contribution). The interferometric patterns observed in the data set supports the our hypothesis, and it lead us to imagine that Equation 8 is valid only in a certain range of elevations and roughness states, where the reflection is essentially diffuse. The characteristics of such regime would be (1) the reflected signal is not coherent--random phase behavior-- and (2) it is delayed with respect to the specular ray path. Consequently, it should exist a transition between this diffuse regime and the coherent regime. The transition regime (1) would gradually lose coherence and (2) would gradually be delayed with respect to the specular, as elevation rises. This last effect would speed up the interferometric phase, introducing biases and trends in the altimetric solution.

The effect of the roughness is being investigated through simulations of the scattering process under different sea states. The Kirchhoff model is used as in (Beckmann and Spizzichino, 1963):

$$E = i e^{ikR_0} / (4 \pi R_0) \int_S [R \mathbf{v} - \mathbf{p}] \cdot \mathbf{n} e^{i\mathbf{v} \cdot \mathbf{r}} dS \quad [9]$$

Where R_0 is the distance from the transmitter to the specular point; R is the Fresnel scattering coefficient for circular polarization (co-polar and cross-polar tested); $\mathbf{v} = \mathbf{k}_{inc}$

k_{sct} ; $p=k_{inc}+k_{sct}$ and n is the unitary vector normal to the sea surface, S . The incoming signal is modeled at GPS L1 frequency modulated with coarse PRN code (C/A code). The sea surface is generated through the two dimensional spectrum in (Elfouhaily et al., 1997) for developed seas, and later mounted on a round Earth. Results in this paper correspond to a patch of 2000 m along the scattering direction and 100 m across it, gridded at 10 cm spacing for the electromagnetic integration. The simulation tool has been validated using flat surfaces. A set of surfaces of equivalent statistical properties and the electromagnetic response on them are being generated to separate particular features from statistical ones, and the effect of the shadowing of the surface's waves is also being considered (not ready at the time of this proceedings).

Figure 5 displays the values of the amplitude and phase of the Kirchoff integrand at each point on the surface. It shows how the roughness destroys the fresnel zone and splits it into independent pieces that may introduce multipath (diffusion regime).

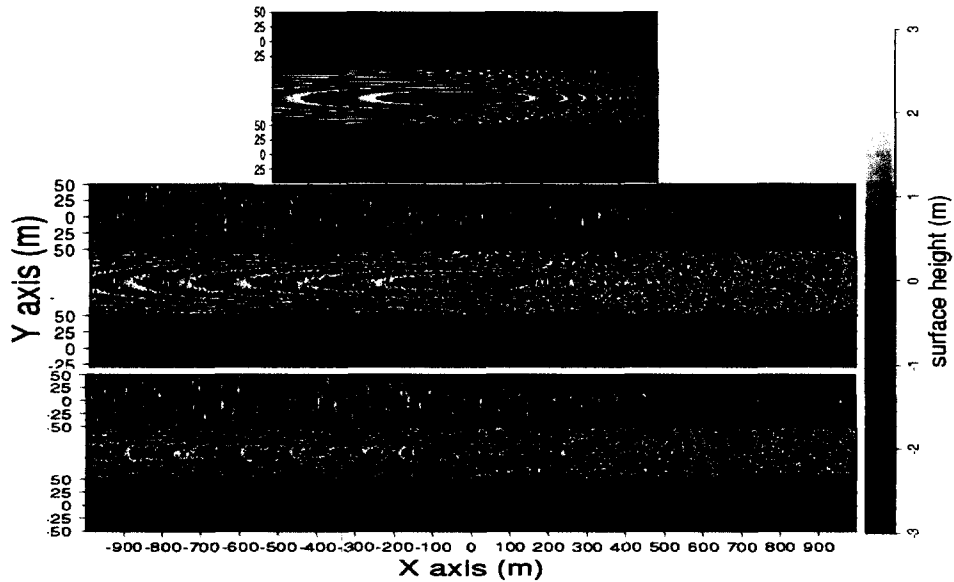


Figure 5: Effect of the roughness on the electromagnetic field. Each 3-plot set contains a map of the sea surface elevation (lower, color scale on the right); amplitude of the surface-cell contribution (higher, arbitrary units) and phase of the field contribution due to each surface-cell (middle, 1 BW transition for 1 cycle). The elevation angle of observation is 3 degrees in all cases, whereas the roughness changes from SWH=0 (flat surface check, higher triplet), SWH=0.6 m (triplet in the middle) and SWH=2.6m (lower triplet). The Fresnel zones on the flat surface are gradually destroyed with the roughness, generating a set of stationary-phase zones delayed with respect to the specular ray. These plots qualitatively describe the transition from the coherent regime to the diffuse regime, and explain the additional delay introduced by the roughness.

The behavior of the interferometric phase in elevation, for each case in Figure 5 is displayed in Figure 6. While the interferometric phase produced by a reflection on the gently rough surface (SWH=0.6 m) has a net slope as the flat surface (meaning that no biases or trends would be introduced in the altimetric product, only unbiased noise), the reflection off 2.6 m sea waves speeds up the interferometric phase with a net increment

of ~50 degrees (2.6 cm slant, 0.5 m vertical) in 0.05 degrees (usually scanned in ~6 seconds). According to these results, if the 2.6 m roughness effect is not corrected, it would introduce a trend in the altimetric solution of 0.5 m in 6 seconds (at 3 deg elevation). Taking into account that a variation in elevation from 3 to 3.05 degrees represents ~25 m displacement on the sea surface, a distance shorter than the main wavelength of the rough surface (~100 m from Figure 5), this feature could only be a partial scanning of the waves, with no net effect after longer elevation variations. The lack of simulations on more surfaces of equivalent roughness properties makes difficult to conclude whether the features captured on this Figure are particular to the simulated surface or representative to the statistical roughness.

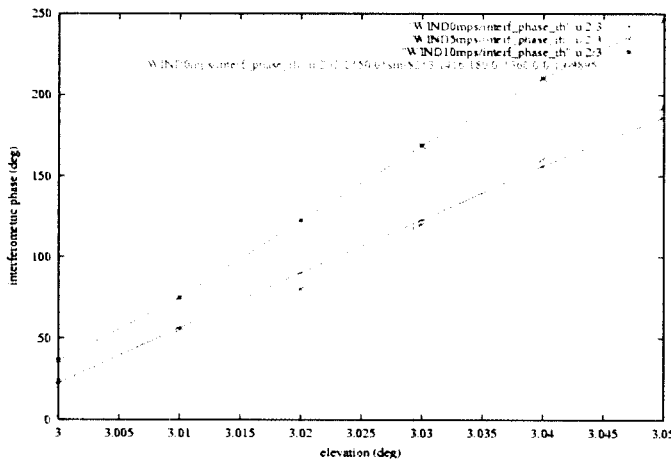


Figure 6: Interferometric phase from simulated scattering on rough surfaces. (pink) as expected from specular reflection (except a bias); (red) simulated on a flat surface; (green) simulated on a surface with waves of SWH=0.6 m; (blue) on SWH= 2.6 m. While the net slope of the green solution follows the flat model (no biases/trends on the altimetric solution), the blue one speeds up the interferometric phase, resulting a trend in the vertical altimetric solution of 0.5 m on ~6 seconds (partial scanning of particular surface?).

5. Carrier phase altimetry

30 seconds of PRN13 data were post-processed to acquire the interferometric phase. The procedure is the same described in (Treuhaft et al., 2001), where the complex delay-waveforms are fitted onto the direct+specular total field model in Equation 2 to infer the interferometric phase $ko(rr-rd)$. A phase ambiguity term ($+n$, being n an integer number of cycles) is added to Equation 3, which is then applied in 20 ms batches to estimate the time series of the altitude (finally expressed in length units). The tropospheric correction is taken from climatologic values together with mapping functions (Neill, 2000). The inaccuracy of such standardized correction introduces an offset to the solution, acceptable for the purposes of the study (to assess about the feasibility of the technique and design the inversion algorithm). The cycle ambiguity resolution (value of n) is obtained by comparison of the resultant altitudes for several possible values of n , with respect to the coarse estimation from the frequency analysis, Table 1. This is possible because the accuracy of the coarse estimation is within the cycle resolution at low elevation ($\Delta H_{cycle} = \lambda / (2 \sin(el))$). As displayed in Figure 7, this technique allows carrier-phase altimetry with rms=0.16 in 100 m of horizontal scanning (15 seconds), which represents $\sigma \sim 1$ cm precision over 100 m of horizontal scale if we

can consider independent individual measurements. The potential roughness information content in the rms scatter (slow frequency noise) is still to be investigated.

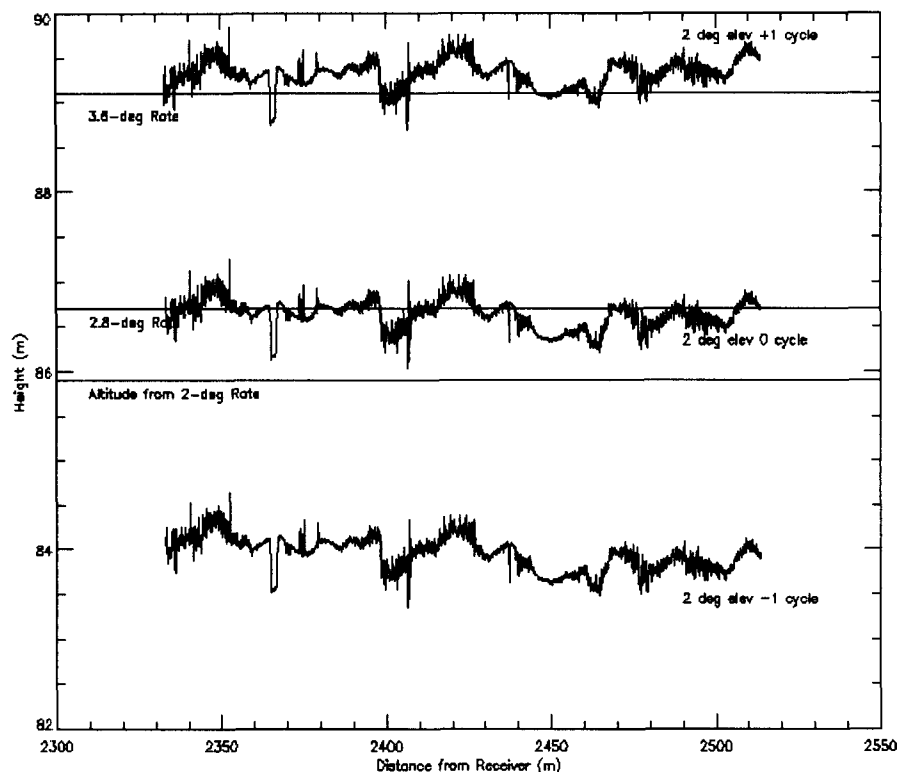


Figure 7: Carrier-phase altimetry for 30 seconds of PRN13 at ~ 2 degrees elevation. The cycle ambiguity is resolved from the coarse estimation of the altitude from the frequency analysis (Table 1), that is: when we add or subtract a cycle, the solution in altitude jumps out of the coarse solution accuracy. The precision of the measurement is of the order of 1 cm in 100 m horizontal. The slow frequency noise (rms 0.16 m, periods of several seconds) may be due to the surface roughness (to be investigated). This particular solution may be biased because of the inaccurate tropospheric correction, which limits the accuracy of this technique.

We suggest, thus, the main steps of a new algorithm for unambiguous carrier-phase altimetry at low elevation angles of observation. The first step is the frequency analysis of the amplitude of the total received field (direct+reflected) to obtain a coarse estimation of the altitude; the second is the computation of corrections (troposphere, roughness, more investigation required); the third step is the inversion of the delay-waveforms to interferometric phase, and finally, the inversion of the phase into the altimetric product, making use of the coarse altitude solution (step 1) to solve for the cycle ambiguity. The accuracy of such technique is driven by the accuracy of the corrections, since the tracking accuracy has been successfully solved.

6. Conclusions

This paper presented the potential use of the GPS reflections at low elevation angles for carrier-phase altimetry. We first showed the coherent or specular nature of such a scattering geometry from the interferometric fringe detected in data collected from a coastal ground station at 85 m nominal altitude. The effects of both tropospheric gradients and roughness into the interferometric parameters are being investigated through forward ray tracing techniques and simulations of the electromagnetic scattering onto realistic surfaces. We have also introduced the interferometric frequency as a valid source for a coarse estimation of the altimetric range, with accuracy better than the vertical projection of one carrier cycle. After the processing to obtain carrier-phase observables and inversion to vertical height, this coarse estimate is then used to solve for the cycle ambiguity intrinsic to this kind of measurements. This completes the main steps of a new algorithm to do altimetry from GPS reflections at low elevation, with precision of the order of 1 cm in 15 seconds (100 m horizontal scanning at 2 deg observations) and accuracy solely limited by the quality of the tropospheric and roughness corrections.

Acknowledgments

The research described in this paper was carried out by the Jet Propulsion Laboratory, California Institute of Technology, under contract with the National Aeronautics and Space Administration and a NASA funded National Research Council associateship program.

References

- Beckmann, P. and A. Spizzichino, The scattering of electromagnetic waves from rough surfaces, Pergamon Press, 1963.
- Beyerle, G., K. Hocke, J. Wickert, T. Schmidt, C. Marquardt and C. Reigber, GPS radio occultations with CHAMP: a radio holographic analysis of GPS signal propagation in the troposphere and surface reflections, *Journal of Geophysical Research*, Vol.107, No.D24, 4802, doi:10.1029/2001JD001402, 2002.
- Cardellach, E., G. Ruffini, D. Pino, A. Rius, and A. Komjathy, 2003, Mediterranean Balloon EXperiment: GPS reflections for wind speed retrieval from the stratosphere. *Remote Sensing and Environment*, accepted July 2003.
- Elfouhaily, T., B. Chapron, K. Katsaros, and D. Vandemark, 1997, A unified directional spectrum for long and short wind-driven waves, *J. Geoph. Res.*, vol 102, no. C7, p. 15,781--1,796, 1997.
- Elfouhaily, T., D.R. Thompson and L.Linstrom, Delay-Doppler Analysis of Bistatically Reflected Signals From the Ocean Surface: Theory and Application, *IEEE Transactions on Geoscience and Remote Sensing*, 40(3), 560-573, 2002.
- Garrison, J.L, A. Komjathy, V.U. Zavorotny and S.J. Katzberg, Wind Speed Measurements Using Forward Scattered GPS Signals, *IEEE Trans. Geosc. Remote Sensing*, Vol. 40, No.1, January 2002.

- Lowe, S.T., J.L. LaBrecque, C. Zuffada, J.L. Romans, L.E. Young, and G.A. Hajj, First spaceborne observation of an Earth-reflected GPS signal, *Radio Science*, Vol. 37, No. 1, 10.1029/2000RS002539, 2002.
- Lowe, S.T., C. Zuffada, P. Kroger and L.E. Young, 5-cm precision aircraft ocean altimetry using GPS reflections, *Geophysical Research Letters*, Vol.29, No.10, 10.1029/2002GL014759, 2002.
- Martín-Neira, M., 1993, A passive reflectometry and interferometry system (PARIS): application to ocean altimetry, *ESA Journal*, vol 17, pp 331-355.
- Martín-Neira, M., M. Caparrini, J. Font-Rossello, S. Lannelongue, and C. Serra Vallmitjana, The PARIS Concept: an Experimental Demonstration of Sea Surface Altimetry Using Reflected GPS Signals, *IEEE Trans. Geoscience and Remote Sensing*, vol. 39, no. 1, 2001.
- Niell, A.E., Improved atmospheric mapping functions for VLBI and GPS, *Earth Planets Space*, 52, 699-702, 2000.
- Rius A., J.M. Aparicio and E. Cardellach, Sea surface state measured using GPS reflected signals, *Geophysical Research Letters*, Vol.29, No23, 2122, doi: 10.1029/2002GL015524, 2002.
- Treuhaf, R.N., S.T. Lowe, C. Zuffada and Y. Chao, 2-cm GPS altimetry over Crater Lake, *Geophysical Research Letters*, Vol.22, No23, 4343-4346, December 2001.
- Zavorotny, V.U., and A.G. Voronovich, A.G., Scattering of GPS Signals from the Ocean with Wind Remote Sensing Application, *IEEE Transactions on Geoscience and Remote Sensing*, Vol. 38, No. 2, pp. 951-964, 2000.